THESIS FOR THE DEGREE OF LICENTIATE OF ENGINEERING

Kinetic modeling for catalytic upgrading of biomass-derived raw gas produced in dual fluidized bed gasifier: An application with ilmenite as the catalyst

HUONG N. T. NGUYEN

Department of Energy and Environment
CHALMERS UNIVERSITY OF TECHNOLOGY
Gothenburg, Sweden 2016

Kinetic modeling for catalytic upgrading of biomass-derived raw gas produced in dual fluidized bed gasifier: An application with ilmenite as the catalyst

HUONG N. T. NGUYEN

Department of Energy and Environment
Chalmers University of Technology
SE-412 96 Gothenburg
Sweden
Telephone + 46 (0) 31 772 1000

Chalmers Reproservice
Gothenburg, Sweden 2016

Kinetic modeling for catalytic upgrading of biomass-derived raw gas produced in dual fluidized bed gasifier: An application with ilmenite as the catalyst

HUONG N. T. NGUYEN
Division of Energy Technology
Department of Energy and Environment
Chalmers University of Technology
SE-412 96 Gothenburg, Sweden

Abstract

Biomass gasification to convert biomass into an energy-rich raw gas is an attractive technology to reduce CO_2 emissions and dependence upon fossil fuels. However, the raw gas contains tar, which comprises condensable organic compounds that can disrupt downstream processes, thereby limiting direct applications of the raw gas. Thus, the removal of the tar is a prerequisite for process viability. Among the currently available methods for secondary tar abatement, catalytic gas cleaning is particularly interesting. The method enables recovery of the chemically stored energy in the tar, and the stable tar species can be efficiently eliminated at a considerably lower temperature than that is required by inert thermal methods. To optimize the gasification and integrated processes, kinetic modeling of the catalytic upgrading of the raw gas is essential.

The aim of this work is to develop a kinetic approach that describes the evolution of tar and light hydrocarbons throughout the catalytic gas cleaning process. In particular, focus is a raw gas that is produced in a dual fluidized bed gasifier, and that contains a high content of light hydrocarbons and tar dominated by aromatic species. As the first step, the mechanism that encompasses the principal trends in the evolution of tar and light hydrocarbons is formulated. Thereafter, using this mechanism and a pseudo-tar that represents tar and light hydrocarbons formed in situ, a kinetic model is developed. To demonstrate the applicability of the kinetic model, process-activated ilmenite is used as the catalyst for the gas cleaning process. The effects of ilmenite on the tar decomposition and gas composition were evaluated at 800°C for three different gas-solid contact times. The experiments were conducted in a bench-scale, bubbling fluidized bed reactor that was fed with a biomass-derived raw gas from the Chalmers dual fluidized bed gasifier operated at 820°C. Combining the experimental results and the kinetic model, the evolutionary profiles of the different tar and light hydrocarbon groups in relation to gas-solid contact time are elucidated. These profiles provide more insights into the conversion of tar and light hydrocarbons in a general catalytic gas cleaning process.

To identify the contributions of steam reforming, dry reforming, and hydro-cracking reactions to the conversion of tar and light hydrocarbons in the gas cleaning process using ilmenite as the catalyst and to define the most important reactions to be accounted for in the kinetic modeling, a second experimental investigation was conducted. The raw gas from the Chalmers gasifier was used as the reference. Representative reactions associated with the cleaning process of the given

raw gas were identified and investigated independently to examine their individual effects. The reactions were then re-combined to investigate the synergistic effects. The temperature range of 750–900°C was used. The complete steam reforming, steam dealkylation, and hydro-cracking reactions were found to have significant impacts, while the contribution of the dry reforming reaction was minimal. Furthermore, the water-gas shift was found to play a significant role and could promote the hydro-cracking reaction.

List of publications included in the thesis

I. Huong N. T. Nguyen, Nicolas Berguerand, Henrik Thunman. Mechanism and kinetic modeling of catalytic upgrading of a biomass-derived raw gas: An application with ilmenite as catalyst. *Industrial & Engineering Chemistry Research 55, pp. 5843-5853, 2016*.

II. Huong N. T. Nguyen, Nicolas Berguerand, Georg L. Schwebel, Henrik Thunman. Importance of decomposition reactions for the conversion of tar and light hydrocarbons using ilmenite as catalyst. *Submitted to Industrial & Engineering Chemistry Research*.

Author details

Huong N. T. Nguyen is the principal author of paper I and II. Dr. Georg L. Schwebel contributed to experimental work, discussion and editing paper II. Assistant Professor Nicolas Berguerand, who is the assistant academic supervisor, participated in experimental work, contributed to discussion, and edited the papers. Professor Henrik Thunman, who is the principal academic supervisor, contributed ideas, discussion and editorial support to the papers.

List of publications not included in the thesis

I. Huong N. T. Nguyen, Nicolas Berguerand, Henrik Thunman. Process activated ilmenite as catalyst for cleaning of biomass producer gas. *4th International Symposium on Gasification and its Applications (iSGA-4), Vienna, Austria, 2014*.

II. Huong N. T. Nguyen, Nicolas Berguerand, Henrik Thunman. Process activated ilmenite as catalyst for cleaning of biomass producer gas. *3rd International Conference on Chemical Looping, Gothenburg, Sweden, 2014*.

Acknowledgment

First of all, I would like to express my sincere gratitude to my academic supervisor Henrik Thunman. To me, you are the best coach who always guides me to a bright spot whenever I feel stuck. Thank you for your enthusiasm and time that you have dedicated for supervision. I would like to give my grateful thanks to Nicolas Berguerand, my assistant academic supervisor. Thank you for your great support in experimental works and for super-quick responses in my writing tasks. I would like to thank Georg Schwebel, who to me is also a supervisor. Thank you for teaching me to become a real engineer. I would like to thank Fredrik Lind for all helps and discussions. I have learned a lot from you as well. To Martin Seemann and Fredrik Normann, thank you so much for your eager discussions about my research.

I would like to thank Jessica Bohwalli, Johannes Öhlin, Rustan Hvitt and the operating staff at Chalmers Kraftcentral (KC). On top of all great helps you have done, I am certain that my successful experiment day is only a small step ahead, just because you are being in KC.

I would like to thank all my great colleagues in Gasification group and in Environmental Inorganic Chemistry group. I am proud of being part of our groups. My special thanks go to Teresa, Jelena, Mikael, Sébastien, Golnar, Martin, Dazheng and Dongmei for all helps along with experiments and for fruitful discussions. I would like to thank everyone at the Division of Energy Technology for that you have created the best ever working environment. To my officemate Tove, thank you for being always willing to fill my understanding about Sweden.

Thank you Ngu-ồn A1 for being an indispensable part of my life. We have been together for 14 years, and we will be for longer. To my childhood friends Tuyết Giang and Vĩnh Phương, thank you for always supporting me no matter what would have happened. You make me realize that true friendship never grows old. To Kim Phượng, Thoa, Chi, Huyền, Diễm, Svetlana, Julie and Hedy, thank you for being my dear friends. To all Vietnamese ‘‘anh, chị, bạn, em’’ I have met in Sweden, thank you for that you warm up my spiritual life and make me feel like I am being at home. To my sister-friend Mai, thank you for caring for me and sharing coincidentally similar perspectives on life.

Last but not least, I would like to give my gratefulness to my parents and my brother. Thank you for always being my greatest support. You bring me back to life and make me believe that ‘Sau cơn mưa, trời sẽ lại sáng’ (After the rain, there will be always the sun).

This work has been financially supported by E.ON and the Swedish Gasification Centre (SFC). Operation of the gasifier was supported by Göteborg Energi, Metso, Akademiska Hus, and the Swedish Energy Agency.

Huong Ngoc Thuy Nguyen

Gothenburg, August 2016

Table of contents

1. Introduction

Biomass gasification is a thermochemical process that converts biomass into an energy-rich raw gas. Heat is supplied to the process through either the combustion of part of the input fuel or other means, such as circulation of hot bed material. In addition, air, oxygen, steam or mixtures thereof are used as oxidants, so-called gasifying agents. As a whole, the gasification process yields a raw gas, which consists mainly of: steam; permanent gases H_2, CO, CO_2, CH_4, and other light hydrocarbons (HC); and condensable organic compounds, known as tar. Ash and other inorganic contaminants, such as NH_3, H_2S, and HCl, may also be present in the raw gas, depending on the composition of the biomass feedstock.

As the raw gas can have various applications, biomass gasification represents an attractive technology for reducing CO_2 emissions and current dependence on fossil fuels [1-3]. The raw gas can be burned directly to produce heat or it can be integrated with gas turbines or fuel cells to produce electricity. Furthermore, it can be used for the synthesis of high-grade products, such as methane, methanol, Fischer-Tropsch fuels, and other chemicals. However, unless the raw gas is burned directly after production, the levels of the contaminants in the raw gas, which include particles, inorganic matter, and tar, must be reduced to levels that are specified according to the envisaged end-use of the raw gas [4]. In particular, the removal of tar plays a key role, not only in maintaining continuous process operation, but also in improving process efficiency. Indeed, tar can already condense at about 350°C, which can cause fouling or plugging of pipe systems, filters, compressors, and other equipments downstream of the gasifier. Furthermore, the chemically stored energy in tar can account for up to 15% of the energy content of the dry ash-free biomass feedstock. Thus, the tar fraction contributes significantly to the cold gas efficiency of the gasification process [5-7].

Considerable efforts have been dedicated to reduce the tar content in the raw gas. The tar yield of the gasification process, to a great extent, depends on the gasifier design, gasifying agent, biomass feedstock and operating conditions such as temperature, pressure, and amount of gasifying agent in relation to amount of biomass feedstock [1, 5, 8]. Thus, reduction of the tar yield can be achieved by optimizing the above-mentioned parameters. Another strategy to reduce the tar yield in fluidized bed gasifiers is to use catalytic bed materials instead of inert silica sand [8-10]. In this case, the agglomeration and oxygen transport capacities of the bed materials have to be carefully considered, so as to maintain continuous process operation and preserve a relatively high heating value of the raw gas [9-11]. Ideally, using in-bed catalysts, the number of reactors required for secondary tar cleaning downstream of the gasifiers is reduced. However, additional secondary measures for tar removal are often required to lower further the tar content, which is especially crucial for the synthesis of high-grade products where the catalysts used for the syntheses can easily be deactivated by the tar [6, 12].

The secondary measures for tar removal can follow three main approaches: physical separation; inert thermal gas cleaning; and catalytic gas cleaning [2, 6, 13, 14]. Among the available physical methods, wet scrubbing is widely employed owing to its competitive efficiency and investment cost, as compared to other physical means, such as cyclones and wet electrostatic precipitators [15,

16]. Generally, water or organic scrubbing media such as rapeseed methyl ester (RME) are used as absorbents to remove tar from the raw gas. Subsequently, the tar-laden scrubbing solvent can be burned to produce heat in a combustion site or it can be re-injected into the gasifiers for further conversion. However, the wet scrubbing method faces both economic and environmental challenges. These challenges relate mainly to wastewater treatment, recycling of the scrubbing solvents, and a potential thermal penalty associated with the substantial levels of gas cooling and reheating required for the subsequent gas conditioning or synthesis [15, 17].

In thermal and catalytic gas cleaning systems, the tar is chemically converted into more desirable gas products, such as methane, CO, and H_2, instead of being physically removed. The cold gas efficiency of the gasification process is thus increased by the addition of chemically stored energy from the tar fraction [2, 6, 18, 19]. The inert thermal method is suitable for eliminating thermally unstable tars, such as oxygenated components. However, for eliminating stable tars, such as aromatic HC, a high operating temperature of about 1100°C and oxygen addition (for partial tar oxidation) are often required [6, 12, 20, 21]. In contrast, catalytic gas cleaning is performed in the presence of a catalytic material, thus requiring lower temperatures, i.e., in the range of 700–900°C, to decompose efficiently the stable tars [2, 4]. Furthermore, the composition of the upgraded gas, particularly the H_2/CO ratio, can be catalytically adjusted *via* the Water-Gas Shift reaction (WGS), which offers advantages for downstream synthesis steps, such as methanation [2, 6].

To optimize the gasification and the integrated processes, kinetic modeling of the evolution of tar during the catalytic gas cleaning is particularly important. However, it is difficult to propose a comprehensive mechanism and kinetic model to describe the entire process owing to the inherently complex compositions of the raw gas and tar, as well as the complicated pathways of simultaneous and consecutive reactions. In the literature, the kinetics of secondary catalytic tar decomposition are often modeled using single-compound approaches or lump models [7]. In the single-compound approaches, single stable components, such as benzene, toluene, and naphthalene, are investigated individually, which means that the kinetic parameters are derived only for the studied tar species [22, 23]. In contrast, the lump models consider all the tar species that are present in the raw gas, which is more practical, as compared to the single-compound approach. Corella et al. [24-26] have suggested several lump models in which gradual improvements were made to take into account the different reactivities of the various tar groups, and the conversion pathways between them. However, some shortcomings remain. First, the facts that heavier tar components can be formed from lighter fractions and that the gas species can interact to form tar are not considered. Second, the roles of steam, H_2, and CO_2 as reforming/cracking agents are not adequately incorporated into the modeling. Third, the available models focus solely on the tar, and only the major conversion pathways among the tar groups are taken into account. The evolution of light HC is not included in the model, even though the light HC can be present in significant amounts in the raw gas and their reactions may make important contributions to the overall process. This is especially important for raw gases that containing large fractions of methane and other light HC [5, 27].

Aims of the work

The aims of this work are to: (i) formulate a reaction mechanism that would improve current understanding of the principal evolutionary routes of tar and light HC; and (ii) develop a kinetic model that could sufficiently capture the main features of the catalytic gas cleaning process and define the evolutionary profiles of the different tar and light HC groups. The raw gas produced by the Chalmers 2–4-MW dual fluidized bed biomass gasifier operated at 820°C was used for the following reasons: (i) as steam is used as the gasifying agent, the raw gas contains high levels of steam and H_2, and the tar yield is higher than is for a bubbling fluidized bed gasifier that uses oxygen or air as the gasifying agent, which makes it easier to take into account the roles of reforming/cracking agents and to visualize the tar evolution [1, 6, 28]; (ii) stable aromatic tar predominates and is suitable for kinetic modeling of the catalytic tar decomposition [25, 26]; and (iii) methane and other light HC, such as ethene, are present in significant amounts. Finally, to demonstrate the kinetic approach, an ilmenite ore with moderate catalytic activities towards tar and light HC conversion was used, with the goal of achieving a gradual evolution of tar and light HC in relation to the gas-solid contact time.

Structure of the thesis

This thesis is organized as follows. After this Introduction, Chapter 2 provides a selective review from the literature on the maturation, sampling, and analysis of the tar, as well as the catalytic cleaning method for tar removal. Chapter 3 introduces the mechanism and kinetics that describe the evolution of tar and light HC during the catalytic raw gas upgrading. Chapter 4 describes the selection of ilmenite as the catalyst to demonstrate the applicability of the kinetic approach. Chapter 5 is the experimental section, in which the operating conditions for the Chalmers biomass gasifier and the composition of its raw gas, as well as the experiments using ilmenite as the catalyst for secondary gas cleaning are summarized. Chapter 6 presents the main results, in particular the evolution of tar and light HC, and the contributions of steam reforming, dry reforming, and hydro-cracking reactions to the catalytic gas cleaning process using ilmenite are discussed. The main conclusions drawn from the obtained results are outlined in Chapter 7. Finally, suggestions as to future studies are put forward in Chapter 8.

2. Background

2.1. Tar

As introduced above, tar consists of condensable organic compounds. During the gasification of a biomass particle, tar is initially formed as part of the pyrolysis that initiates at approximately 200°C. During this pyrolysis, cellulose, hemicellulose, and lignin in the biomass are converted into smaller molecules, including primary tar. Oxygen-rich compounds, such as carboxylic acids, ketones, alcohols, and aldehydes, are the main components of the primary tar class. After the primary tar is formed, it evolves depending on the process operating conditions, such as temperature, residence time of the raw gas inside the gasifier, and the nature of the contacts between the tar and gasifying agents, all of which influence the final tar composition. Generally, at temperatures >500°C, primary tar is decomposed into permanent gases and secondary tar, which is itself characterized by phenolic components. At temperatures around 700°C, secondary tar is the dominant tar species in the resulting raw gas. However, at higher temperatures, secondary tar is further converted into permanent gases and tertiary tar, which consists of stable aromatic HC [4, 6, 15, 29-31].

The tar content of the raw gas is a key indicator of the performance of the gasification process, and the end-uses of the raw gas require that the tar composition is known. Thus, tar sampling and analysis are important. Both offline and online methods for tar measurement have been developed, with the offline methods being more widely used and mature [6, 7, 32, 33]. Cold Solvent Trapping (CST) and Solid Phase Absorption (SPA), which are the two most commonly used offline methods, are discussed here. The CST method is based on the absorption of tar in organic solvents, such as 2-propanol and acetone. After the tar sampling is completed, the solvent and steam are evaporated, and the condensed tar can be weighed to determine the tar content of the raw gas. The tar solution can also be analyzed using, for example, gas chromatography with flame ionization detector (GC-FID), which provides details as to the tar composition. However, due to long sampling times of up to 1 hour, the CST method creates problems with following the gasification process, particularly if one wants to synchronize the tar results with the results of permanent gas analysis for a given measurement point. Furthermore, the dissolved tar and the solvent can mutually evaporate, which may reduce the accuracy of the measurement of highly volatile tar components [7, 34]. In contrast, the SPA method uses solid-phase extraction columns containing solid adsorbents to capture tar. This method has a sampling interval of about 1 minute per sample. Tar is then extracted from the SPA column and the tar-dissolved solvent is further analyzed using GC-FID [35, 36]. SPA columns that contain different types of adsorbents can be used, depending upon the tar species of interest. For instance, the double-layer SPA column, which contains a layer of aminopropyl-bonded silica and a layer of activated carbon, should be chosen if one wants to more accurately quantify the light tars, such as benzene, toluene, xylene, and styrene, in addition to other heavier components. However, if the light tar fraction is not of interest, an SPA column that contains only a layer of aminopropyl-bonded silica can be used [37, 38].

2.2. Catalytic tar removal

2.2.1. Possible reactions

The most relevant reactions associated with the catalytic cleaning process for the tar removal are summarized in Table 1 [4, 39]. For simplification, the general formula for tar in R1–R4 is taken as that of aromatic HC.

Table 1. Reactions during the catalytic cleaning of a raw gas.

Reaction	Formula	
Steam reforming	$C_xH_y + H_2O \rightarrow C_{x'}H_{y'} + CO + H_2$	(R1)
Dry reforming	$C_xH_y + CO_2 \rightarrow CO + H_2$	(R2)
Hydro-cracking	$C_xH_y + H_2 \rightarrow C_{x'}H_{y'}$	(R3)
Thermal cracking	$C_xH_y \rightarrow C_{x'}H_{y'} + C + H_2$	(R4)
WGS	$CO + H_2O \rightleftarrows CO_2 + H_2$	(R5)

The conversion of tar can take place *via* decomposition reactions, which comprise steam reforming, dry reforming, hydro-cracking, and thermal cracking reactions, i.e., R1–R4 in Table 1, respectively. Light HC can also be converted *via* these reaction routes. Note that in R1, in addition to CO and H_2, relatively stable tar/light HC $C_{x'}H_{y'}$ can be formed [27, 40]. Thus, R1 represents either complete steam reforming reaction to produce only H_2 and CO or steam dealkylation. In addition to the decomposition reactions for tar and light HC, the WGS reaction is of great importance, as it can adjust significantly the final composition of the upgraded gas [41, 42].

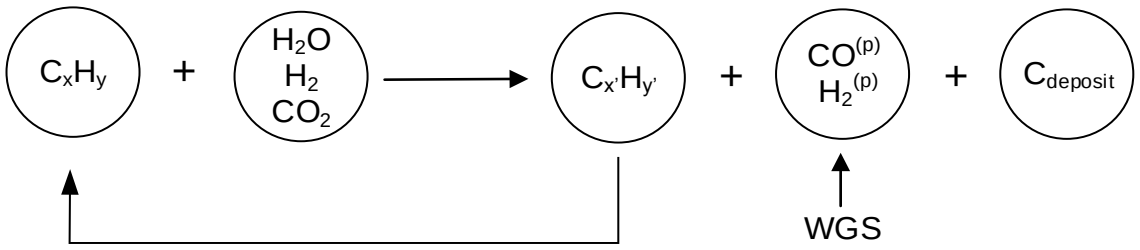

Figure 1. Simplified reaction scheme for a catalytic gas cleaning process.

A simplified reaction scheme to describe a general catalytic gas cleaning process is shown in Figure 1, which aggregates the reactions presented in Table 1. It should be noticed that the concentrations of $CO^{(p)}$ and $H_2^{(p)}$ that are produced from the destruction of tar/light HC are adjusted *via* the WGS reaction. Note that the tar and light HC produced *in situ* $C_{x'}H_{y'}$ can be further converted as the parent tar/light HC C_xH_y.

2.2.2. Catalysts

Various synthetic and naturally occurring catalysts have been investigated for catalytic gas cleaning applications [2, 4, 43]. The aim is to identify catalysts that are: (i) efficient in terms of catalytic activity; (ii) resistant to attrition; (iii) resistant to deactivation by carbon deposits, sulfur, and chloride or easily regenerated from these contaminants; (iv) available at an acceptable price; and (v) environmentally friendly. The most frequently studied catalysts for catalytic gas cleaning applications are listed in Figure 2 [2, 13, 39, 43-47].

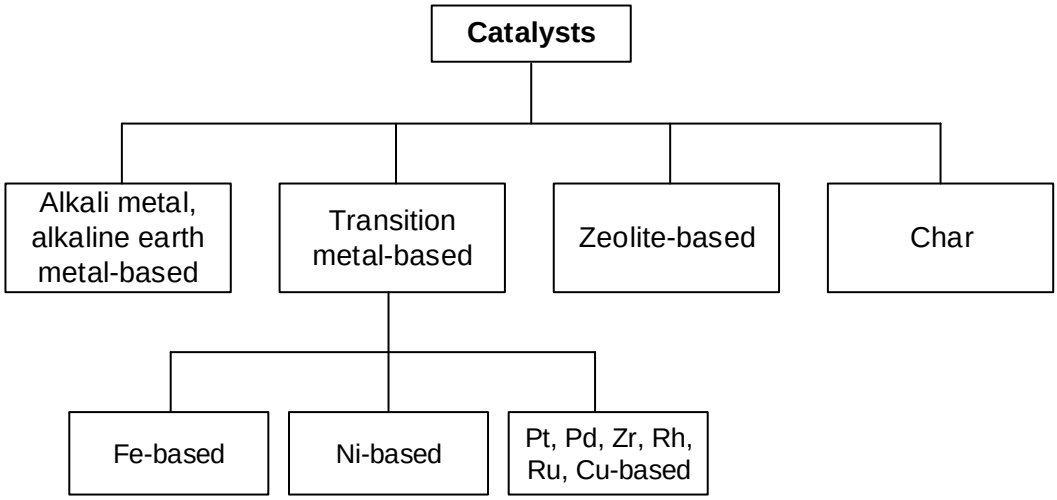

Figure 2. Classification of the most intensively studied catalysts for catalytic gas cleaning applications.

Nickel-based catalysts, which are widely used for naphtha reforming and methane reforming in the petrochemical industry, have been proven to be among the most effective catalysts for raw gas cleaning. However, as nickel is toxic and represents an environmental hazard, its disposal is challenging. Moreover, nickel catalysts are rapidly deactivated by carbon deposits and sulfur [2, 39]. This is, indeed, a common problem for many other catalysts [2, 4, 48]. Extensive studies have been performed on catalyst supports, catalyst promoters, and synthesis methods for the catalysts to suppress the carbon deposits and sulfur [4, 39]. Particularly in the case of metal-oxide catalysts, an alternative solution is to combine continuous tar removal with simultaneous catalyst regeneration [38].

Naturally occurring and inexpensive materials, such as olivine, limonite, ilmenite, and dolomite, are attracting interest, although the catalytic activities of these environmentally friendly catalysts are usually lower than those of nickel catalysts [15, 44, 45]. Char, which is a carbonaceous product that is produced during the pyrolysis of coal and biomass, is also highly interesting in this context [47, 49]. Using naphthalene as a representative tar in CO_2 and steam atmospheres at 900°C, Abu et al. [47] compared the catalytic activities of biomass chars with the catalytic activities of calcined dolomite, olivine, a zeolite-based catalyst, biomass ash, and a commercial nickel catalyst. They found that, after the nickel catalyst, the biomass chars gave the highest

naphthalene conversions (up to 99%). However, in order to incorporate char as a catalyst in a cleaning process for a raw gas, either separated char production or modification of gasifier design is necessary [15]. Furthermore, loss of the catalytic activity of char has to be closely monitored, as the active sites on the char particles are easily blocked by coke deposits [50-52].

3. Mechanism and kinetics of catalytic upgrading of a biomass-derived raw gas

3.1. Mechanism underlying the destruction of tar and light hydrocarbons

A mechanism based on reactive intermediates to describe the catalytic evolution of tar and light HC is outlined in this section. Note that hereinafter, the term 'tar' refers exclusively to benzene and heavier aromatic species, which are particularly in focus in this work. The reactive intermediate-based mechanism reflects the free radical mechanism that has been extensively described for the inert thermal cracking of crude oil and pyrolysis of biomass tar [53-55]. However, herein the general term 'reactive intermediate' is used instead of 'free radical', since the heterogeneous gas-solid phases exist. The reactive intermediates may originate from the reforming/cracking agents steam, CO_2 and H_2, as well as from tar/light HC molecules. These are either free radicals in the gas phase or other intermediates that form and react further on the catalyst surface. In the case of free radicals, they can be created in the gas phase through the thermal effect or on the catalyst surface through the catalytic effect, and desorbed to the gas phase [56, 57]. The rate of formation of reactive intermediates is mainly dependent upon the temperature, catalyst, and the original molecule.

Regarding the reforming/cracking agents steam, H_2, and CO_2, they can be dissociated to produce the hydrogen intermediates H^* and the oxygen-containing intermediates O^* and OH^*, as defined in R6–R8 [42, 54, 58-60].

$$H_2O \leftrightarrows 2H^* + O^* \quad \text{(R6)}$$

$$H_2 \leftrightarrows 2H^* \quad \text{(R7)}$$

$$CO_2 \leftrightarrows CO + O^* \quad \text{(R8)}$$

Similarly, tar/light HC molecules are assumed to be initially converted into reactive intermediates, and it is only in this state that they can react further [42, 61-63]. The gradual destruction of tar/light HC is typically described as follows. Note that the symbols C with subscripts indicate tar/light HC molecules, the symbols C^* with subscripts indicate tar/light HC reactive intermediates, and the subscript letters represent the number of carbons in the molecules or reactive intermediates.

- Tar/light HC molecule self-dissociation:

$$C_x \rightarrow C^*_{x'} + C^*_{x-x'} \qquad C^*_{x'} \text{ is } H^* \text{ if } x' = 0 \quad \text{(R9)}$$

- Interaction between tar/light HC molecules and other reactive intermediates:

$$C_x + H^* \rightarrow C^*_{x-f} + C_f \qquad C_f \text{ is } H_2 \text{ if } f = 0 \quad \text{(R10)}$$

$$C_x + C^*_{x'} \rightarrow C^*_{x+x'-j} + C_j \qquad C^*_{x+x'-j} \text{ is } H^* \text{ if } x + x' - j = 0 \quad \text{(R11)}$$

- Decomposition of tar/light HC intermediates:

$C^*_{x'} \rightarrow C_{x''} + C^*_{x'-x''}$ $\quad C^*_{x'-x''}$ is H^* if $x' - x'' = 0$ (R12)

- Addition of unsaturated HC to reactive intermediates:

$C^*_{x'} + C_q \rightarrow C^*_{x'+q}$ $\quad C_q$ is unsaturated HC (R13)

- Termination:

$C^*_{x'} + H^* \rightarrow C_{x'}$ (R14)

$C^*_{x'} + C^*_u \rightarrow C_{x'+u}$ (R15)

The tar/light HC reactive intermediates are initially generated by: (i) self-dissociation of the tar/light HC molecules; (ii) interactions between tar/light HC molecules and hydrogen intermediates H^*; and (iii) interactions between tar/light HC molecules and tar/light HC reactive intermediates (described in R9, R10, and R11, respectively). It must be emphasized that these initial bond cleavages are assumed to be the rate-determining steps [54, 63, 64]. After formation, the tar/HC reactive intermediates can be decomposed to form smaller species (R12) or they can react with unsaturated HC, such as acetylene C_2H_2, to form larger intermediates (R13). In the termination step, tar/light HC intermediates can react either with hydrogen intermediates H^* to produce relatively lighter products (R14) or with other tar/light HC intermediates to produce relatively heavier products (R15).

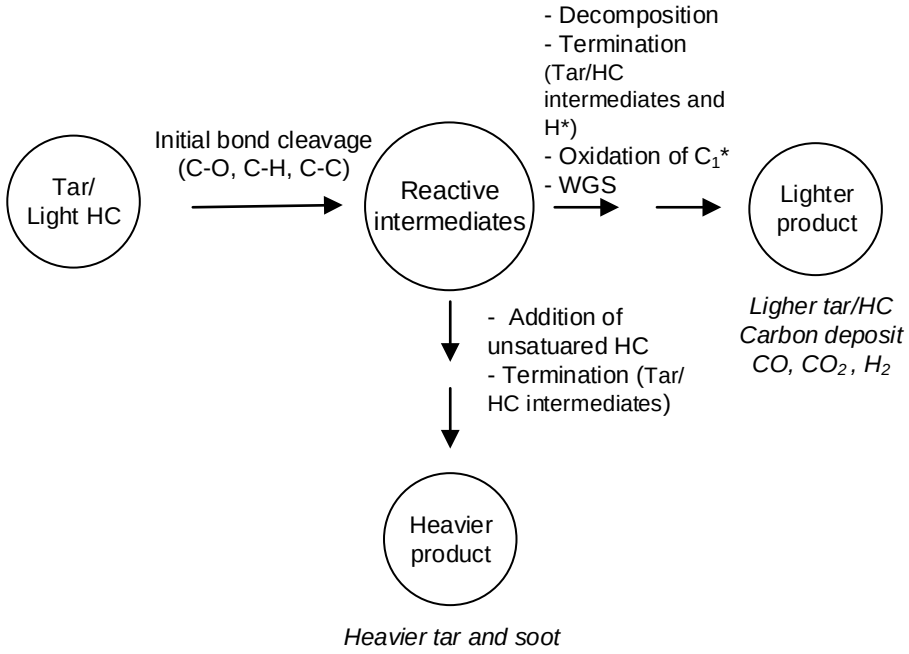

Figure 3. Conversion of tar/light HC molecules and product distributions.

The gradual conversion of tar/light HC and the trends towards producing relatively lighter/heavier products during catalytic gas cleaning are visualized in Figure 3. In addition to what has already been discussed above, it is assumed that once the reactive intermediates that contain only one carbon atom C^*_1 are produced, e.g., after gradual fragmentation (R12), they can

react with available oxidizing agents, such as oxygen-containing intermediates, to produce CO, and thereafter to produce CO_2 *via* the WGS reaction [18, 42, 54, 60].

Expanding upon the information given in Figure 3 in relation to the formation of the lighter products, Figure 4 shows (in a simplified way) the aggregate effects of steam reforming, dry reforming, hydro-cracking, and thermal cracking reactions (reactions summarized in Table 1) on the nature of the carbonaceous products in the upgraded gas. Note that Figure 4 focuses solely on the conversion of aromatic HC tar and light HC in an environment that has a high content of steam, so the formation of relatively larger tar/light HC is not included [37].

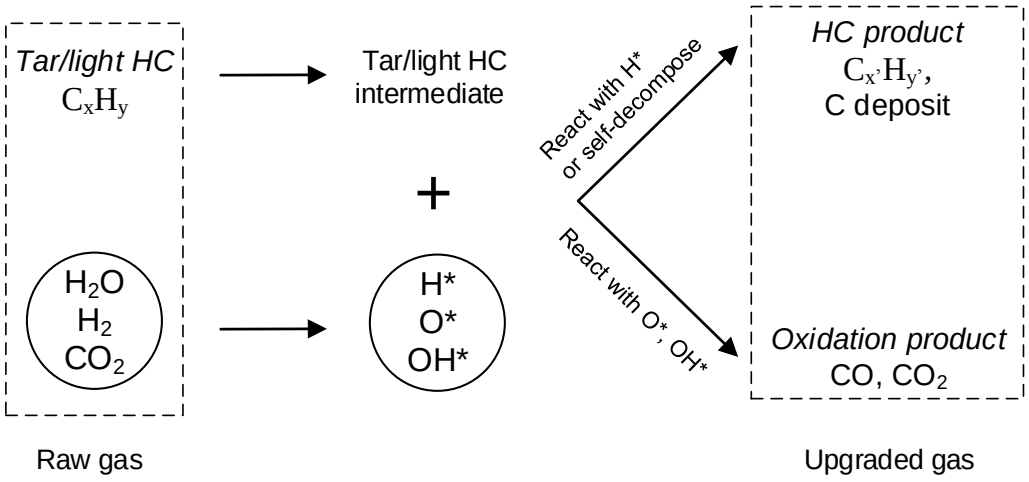

Figure 4. Conversion of tar/light HC under influences of decomposition reactions, and formations of carbonaceous products.

Figure 4 shows that the formation of carbonaceous products, i.e., HC products or oxidation products, depends on whether the tar/light HC intermediates react with hydrogen intermediates or oxygen-containing intermediates. More specifically, the reaction of tar/light HC intermediates with hydrogen intermediates produces another tar/light HC $C_{x'}H_{y'}$, which reflects either the steam dealkylation or hydro-cracking reaction. In contrast, oxygen-containing intermediates oxidize the tar/light HC intermediates to produce CO, and subsequently to produce CO_2 *via* the WGS reaction. This route reflects the effect of either the complete steam reforming or the dry reforming reactions if no other tar/light HC are produced. Finally, the tar/light HC intermediates may self-decompose to produce tar/light HC $C_{x'}H_{y'}$ or carbon deposits, which is the case for the thermal cracking reaction [37, 65]. As the thermal cracking reaction does not require any reforming/cracking agents, the reaction can occur as long as the tar/light HC are dissociated into reactive intermediates. However, this reaction pathway may be negligible if the reforming/cracking agents are present in excess in the reaction environment.

3.2. Kinetic modeling of the evolution of tar and light hydrocarbons

To take into account the differences in reactivity, the tar in the raw gas is categorized into six groups (denoted C1–C6): phenolic and oxygen-containing compounds (C1); benzene (C2); 1-ring compounds (excluding benzene) (C3); naphthalene (C4); 2-ring compounds (excluding naphthalene) (C5); and 3-ring and larger compounds (C6). The general tar formula $C_{x_i}H_{y_i}O_{z_i}$ with specific values of x_i, y_i and z_i for each tar group Ci is defined based on the tar composition of the raw gas. In the same way, light HC are categorized into group C7, which consists of HC in the range of C_2 to C_5 carbons, and the methane group (C8). The general formula $C_{x_i}H_{y_i}$ for group C7 is defined based on the raw gas composition.

The principle of the kinetic model is that a pseudo-tar with the formula of CH_mO_n is introduced to represent all the tar and light HC produced *in situ*. In addition, the rate expression for the time-dependent decomposition of tar/light HC group Ci is formulated for the predefined rate-determining steps, where tar/light HC are initially converted into reactive intermediates, as discussed in Section 3.1. The values of m and n in CH_mO_n are derived from the contents of carbon, hydrogen, and oxygen in the upgraded gas, excluding CO, CO_2, and H_2. CH_mO_n can be produced from the destruction of tar/light HC, as well as from the gas species CO and H_2. After its formation, CH_mO_n is distributed to all the tar and light HC groups. The formation and distribution of the pseudo-tar CH_mO_n are summarized in Figure 5.

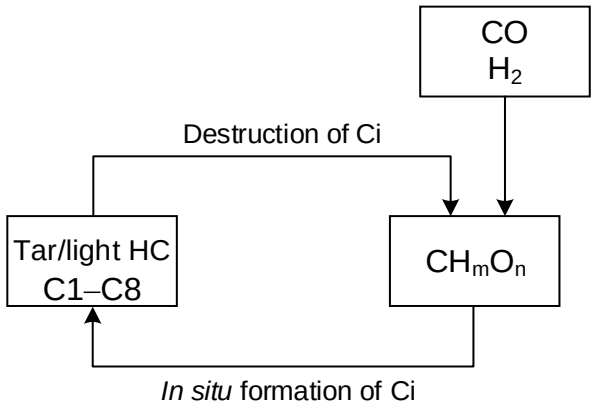

Figure 5. Scheme for the formation and distribution of pseudo-tar CH_mO_n.

The distribution of CH_mO_n to all other tar/light HC groups Ci with the distribution coefficient p_i is given by reaction R16:

In situ tar/light HC formation $$CH_mO_n \rightarrow p_i C_{x_i}H_{y_i}O_{z_i} \quad \text{(R16)}$$

The values of the coefficient p_i satisfy the carbon balance in reaction R16. Moreover, their value ranges can be estimated based on the compositions and molecular structures of the original tar/light HC species in the raw gas.

The rate expression for the time-dependent decomposition of tar/light HC group Ci is written as follows:

$$\frac{dX_{Ci}}{dt} = -\frac{dX_{Ci}(9)}{dt} - \frac{dX_{Ci}(10)}{dt} - \frac{dX_{Ci}(11)}{dt} + p_i S$$
$$= -k_{i9}X_{Ci} - k_{i10}X_{Ci}X_{H^*} - k_{i11}X_{Ci}X_{C^*} + p_i S \quad \text{Eq. (1)}$$

where X_{Ci} is the mole fraction of tar/light HC group Ci [-], X_{H^*} is the mole fraction of hydrogen intermediate H^*[-], X_{C^*} is the mole fraction of tar/light HC intermediate C^*[-], p_i is the distribution coefficient in reaction R16 for tar/light HC group Ci [-], S is the total rate of CH_mO_n formation [s^{-1}], and k_{i9}, k_{i10}, and k_{i11} are the pseudo-kinetic rate constants of elementary reactions R9–R11 with respect to group Ci [s^{-1}].

As shown in Figure 5, the total rate S of CH_mO_n formation has to take into account the levels of CH_mO_n produced from the destruction of the tar/light HC and from the gas species CO and H_2. To enable the estimation of S, the relative levels of CH_mO_n and CO produced from the destruction of the original tar/light HC must be known. Therefore, the parameter w_i $(0 \le w_i \le x_i)$, which represents the number of carbons in a tar/light HC molecule $C_{x_i}H_{y_i}O_{z_i}$ converted into CH_mO_n, is introduced. Note that the values of w_i depend on the actual catalyst used and other process conditions, such as operating temperature. Finally, the total rate S is estimated according to Eq. (2), in which S_{gas} is the rate of CH_mO_n formation from CO and H_2.

$$S = S_{gas} + \sum_i w_i(k_{i9}X_{Ci} + k_{i10}X_{Ci}X_{H^*} + k_{i11}X_{Ci}X_{C^*}) \quad \text{Eq. (2)}$$

The maximum rate of tar/light HC intermediate C^* formation can be estimated from elementary reaction R9 according to:

$$\frac{dX_{C^*}}{dt} = 2\sum_i k_{i9}X_{Ci} \quad \text{Eq. (3)}$$

For a characteristic time-step $\Delta\tau$, the mole fraction X_{Ci} in Eq. (3) can be considered to be constant. Furthermore, the concentration of reactive intermediates can be assumed to be constant throughout the reactions, as the reactive intermediates are much more reactive than the original molecules [65]. Therefore, Eq. (3) can be integrated to give:

$$X_{C^*} = 2\Delta\tau\sum_i k_{i9}X_{Ci} \quad \text{Eq. (4)}$$

Using X_{C^*} from Eq. (4) and further introducing k'_{i11} to replace $k_{i11}\Delta\tau$, Eq. (1) can be rewritten as:

$$\frac{dX_{Ci}}{dt} = -k_{i9}X_{Ci} - k_{i10}X_{Ci}X_{H^*} - 2k'_{i11}X_{Ci}\sum_i k_{i9}X_{Ci} + p_i S \quad \text{Eq. (5)}$$

The rate expression for the mole fraction of H^* versus time is given by:

$$\frac{dX_{H^*}}{dt} = 2k_{f,H_2O}X_{H_2O} - 2k_{b,H_2O}X_{H^*}^2X_{O^*} + 2k_{f,H_2}X_{H_2} - 2k_{b,H_2}X_{H^*}^2 \quad \text{Eq. (6)}$$

where k_{f,H_2O} and k_{b,H_2O} are the pseudo-rate constants in the reversible reaction R6, and k_{f,H_2} and k_{b,H_2} are the pseudo-rate constants in the reversible reaction R7.

To estimate the mole fraction of hydrogen intermediate H^*, two cases are considered that differ with respect to the gas-solid contact time and the catalyst being used: (i) steam and H_2 dissociate insignificantly; and (ii) steam and H_2 dissociate significantly and reach an equilibrium state. In the latter case, the WGS reaction is also at equilibrium. For a given temperature and gas composition, the length of time required for the elementary reactions R6–R8 to reach equilibrium depends on the catalyst used.

For the case in which steam and H_2 dissociate insignificantly, the approximations already applied for the tar/light HC intermediates C^* are used to estimate the mole fraction of hydrogen intermediate H^* from Eq. (6). Moreover, the reverse reactions in R6 and R7 are considered to be slow, as compared with the forward reactions. Finally, using k'_{i10} to replace $k_{i10}\Delta\tau$, Eq. (5) becomes:

$$\frac{dX_{Ci}}{dt} = -k_{i9}X_{Ci} - 2k'_{i10}X_{Ci}\left[k_{f,H_2O}X_{H_2O} + k_{f,H_2}X_{H_2}\right] - 2k'_{i11}X_{Ci}\sum_i k_{i9}X_{Ci} + p_iS \quad \text{Eq. (7)}$$

For the case in which steam and H_2 dissociate significantly and reach equilibrium, the mole fraction of H^* is derived from the expression of the equilibrium constant K_{H_2} for elementary reaction R7. K_{H_2} is incorporated into the pseudo-rate constant k''_{i10} and Eq. (5) is further adapted as follows:

$$\frac{dX_{Ci}}{dt} = -k_{i9}X_{Ci} - k''_{i10}X_{Ci}\,X_{H_2}^{0.5} - 2k'_{i11}X_{Ci}\sum_i k_{i9}X_{Ci} + p_iS \quad \text{Eq. (8)}$$

4. Using ilmenite as the catalyst for secondary gas cleaning

To demonstrate the applicability of the mechanism and kinetics presented in Chapter 3, ilmenite, which is an iron-titanium oxide with chemical formula of $FeTiO_3$, was used as the catalyst. Ilmenite was selected because of the following features:

- The potential of using ilmenite for secondary catalytic gas cleaning has been demonstrated. In addition to its ability to decompose tar, ilmenite can catalyze the destruction of light HC, such as ethene. Moreover, ilmenite significantly induces the WGS reaction [38, 66]. The catalytic effect of ilmenite is largely attributed to its iron content. Moreover, iron is known to chemisorb steam, H_2 and CO_2 [56, 60, 67-69]. Thus, it can be considered that ilmenite facilitates the dissociation of these reforming/cracking agents, and the rate expressions for the destruction of tar/light HC during ilmenite catalysis can be described using Eq. (8).
- In a previous investigation using ilmenite at a gas-solid contact time of about 0.4 s, methane, benzene, and naphthalene were produced to a greater extent than they were reformed [38], which shows that ilmenite has moderate catalytic activity as compared to, e.g., nickel catalysts. Thus, a gradual evolution of tar and light HC in relation to the gas-solid contact time can be expected.
- Carbon deposition is negligible in a high steam-content environment [27, 38, 48].

To induce the reactivity of fresh ilmenite, activation is required. During the activation process, ilmenite has to be exposed to alternating oxidizing and reducing conditions at a temperature of at least 800°C to enhance the porosity and thus, the specific surface area of the ilmenite particles, and to trigger the migration of iron to the particle surface [70, 71]. It must be emphasized that ilmenite possesses both oxygen transport and catalytic capacities. These two different capabilities can be induced exclusively by controlling the redox state of the iron species. More precisely, the oxidized state Fe^{+3} contributes the most to the oxygen transport capacity and the reduced iron species, such as Fe^{+2} and Fe°, are the most active in terms of catalytic activity [8, 65-67]. Thus, for ilmenite to function efficiently as a catalyst, the activation needs to ensure that ilmenite in its reduced form eventually.

5. Experimental section

5.1. Operating conditions for the gasifier and the raw gas properties

5.1.1. Operating conditions for the gasifier

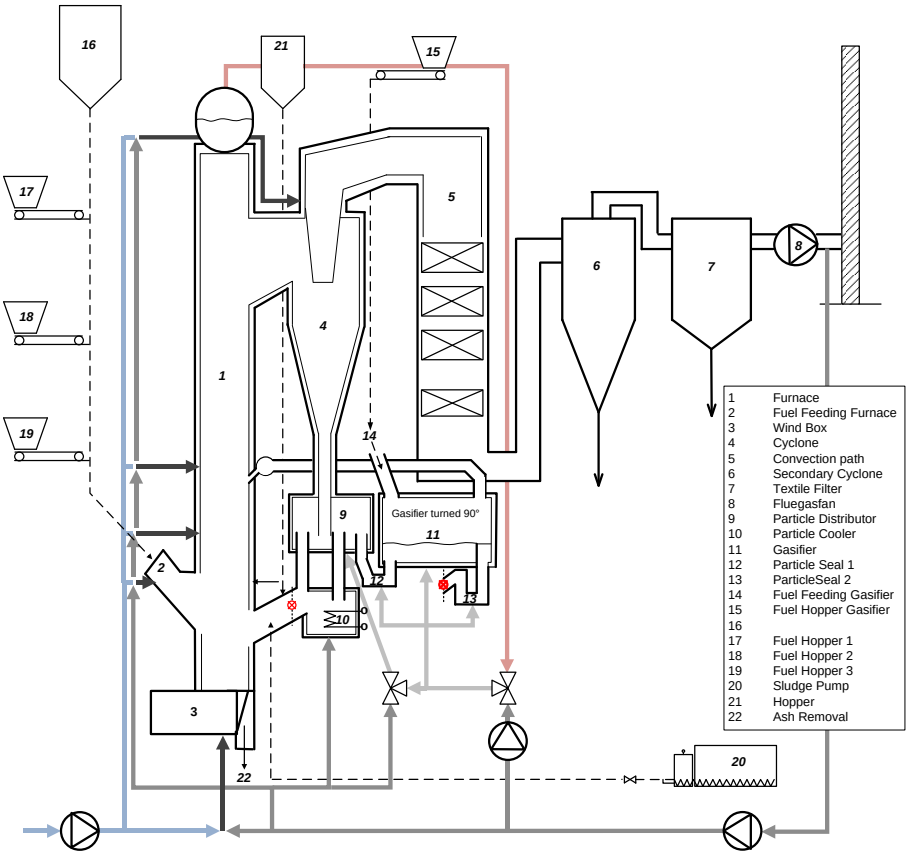

Figure 6. Schematic of the Chalmers combustion-gasifier unit.

In the 12-MW_{th} combustion-gasifier unit installed at Chalmers University of Technology, an indirect biomass gasifier is coupled with a boiler, which is configured as a dual fluidized bed gasifier, as shown in Figure 6. The fuel feed to the gasifier accounts for about 25% of the total fuel load to the whole unit. As the intended purpose of the boiler is to produce hot water for district heating at the Chalmers campus, excess fuel is fed to the boiler. Thus, the heat demand of the gasifier is always fulfilled, irrespective of the operating conditions of the gasifier. Further details of the Chalmers unit are available elsewhere [9, 72].

The conditions applied for operating the gasifier in this work are summarized in Table 2, and the average composition of the wood pellets used as fuel for the gasifier is presented in Table 3.

Table 2. Operating conditions for the gasifier.

Bed material	Silica sand
Total bed inventory (tonne)	3
Temperature (°C)	820
Wood pellet flow rate (kg/h)	300
Steam flow-rate for fluidization in the gasifier (kg/h)	160

Table 3. Ultimate analysis (wt%) of the dry wood pellets.

C	H	O	N	S	Cl	Ash
50.7	6.1	42.7	0.06	~0.02	~0.01	0.4

5.1.2. Raw gas properties

The raw gas contained approximately 60 vol% of steam. The average composition of the permanent gas is presented in Table 4. In addition to the data provided in the table, ethene accounted for approximately 80% of the light HC in the range of C_2–C_3 carbons.

Table 4. Permanent gas composition (vol%)

H_2	CO	CO_2	CH_4	$C_{2-3}H_y$	N_2
28.4	28.7	19.3	12.2	4.9	6.5

The permanent gas composition was analyzed online using the Rosemount NGA 2000 Multi-Component Gas Analyzer and micro-GC Varian 4900. The NGA analyzer measures the concentrations of H_2, CO, CO_2, CH_4, and O_2. The micro-GC, which is equipped with a molecular sieve 5A column and a PoraPLOT Q column that uses Ar and He as carrier gases, measures the concentrations of H_2, CO, CO_2, CH_4, C_2H_2, C_2H_4, C_2H_6, C_3H_6, C_3H_8, N_2, O_2, and He.

For the tar sampling, the SPA method was employed using dual-layer SPA columns that contained a layer of aminopropyl-bonded silica and a layer of activated carbon (Supelclean ENVI-Carb/NH2 SPE tube; Sigma-Aldrich). The detailed procedures for extracting, preserving, and eluting the SPA samples, and the set-up for GC-FID method for tar analysis can be found elsewhere [36]. Note that a temperature ramp from 50°C to 350°C was employed in the GC-FID method to measure tar components ranging from benzene to coronene. The average tar content of the dry raw gas was about 55 g/Nm^3 and the total carbon content of the tar accounted for 11% of the total carbon in the raw gas. The average tar composition is summarized in Table 5. The tar composition was dominated by aromatic HC, and this is attributed to the relatively high operating

temperature of the gasifier, i.e., 820°C, and gas residence time of about 5 s [73]. In particular, benzene, toluene, and naphthalene were the most abundant tar components. Moreover, components that were identified by the GC-FID but only at very low levels, and which as a consequence were not included in the standard tar compounds predefined in the GC-FID method, were designated as 'unknown tar'.

Table 5. Tar composition in the raw gas.

Group	General formula	Composition (wt%)
C1: phenolic and oxygen-containing compounds	$C_{6.77}H_{6.41}O_1$	Phenol: 5.93 o/p-cresol: 1.23 1/2-naphtol: 0.31 2,3-benzofuran: 1.34 Dibenzofuran: 0.62 Xanthene: 0.16
C2: benzene	C_6H_6	Benzene: 33.87
C3: 1-ring compounds	$C_{7.18}H_{8.19}$	Toluene: 11.64 o/p-xylene: 1.49 Styrene: 4.06 Methylstyrene: 1.03
C4: naphthalene	$C_{10}H_8$	Naphthalene: 10.67
C5: 2-ring compounds	$C_{9.79}H_{8.71}$	1,2-dihydronaphthalene: 0.07 1/2-methylnaphthalene: 2.73 Biphenyl: 0.87 Indene: 5.3
C6: ≥3-ring compounds	$C_{13.33}H_{9.22}$	Acenaphthylene: 2.42 Fluorene: 1.02 Phenanthrene: 1.82 Anthracene: 0.53 Fluoranthene: 0.43 Pyrene: 0.43 Chrysene: 0.08
Unknown	N/A	Unknown: 11.95

Finally, it is noteworthy that with the gasifier operating conditions employed in the present study, the yields of light HC in the range of C_4–C_5 carbons and of tars larger than coronene were negligible [73].

5.2. Setup of the experiments using ilmenite

In this work, two experimental investigations were carried out. For the first investigation, ilmenite collected from the fly-ash exiting the Chalmers boiler operated at approximately 900°C (here referred to as 'process-activated' ilmenite) was used [11]. The aim was to evaluate the effects of the process-activated ilmenite on the permanent gas composition and tar decomposition in relation to the gas-solid contact time. The obtained experimental results were used as an input for the kinetic modeling presented in Section 3.2 to derive the evolutionary profiles for different tar and light HC groups during the catalytic gas cleaning process, as well as the conversion network for tar and light HC groups (presented in Section 6.1).

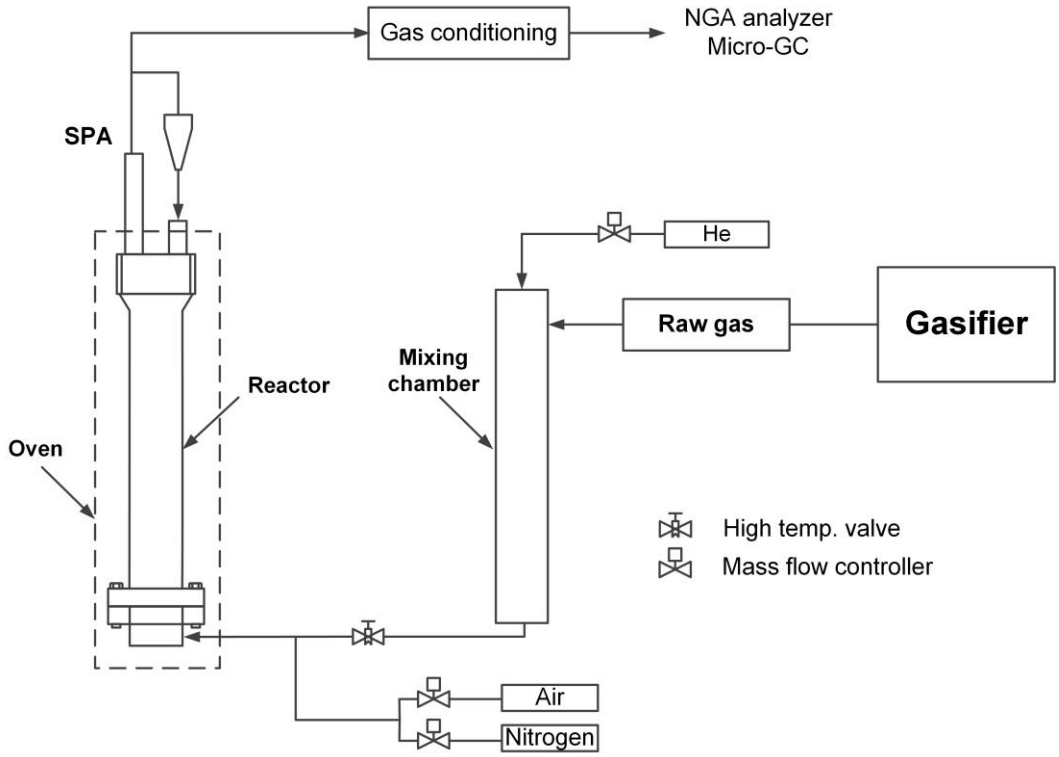

Figure 7. Experimental setup used in the investigation with raw gas from the Chalmers gasifier and process-activated ilmenite.

The experimental setup is shown in Figure 7. The main part of the experimental setup is a batch fluidized bed reactor fed with a slipstream of the raw gas produced in the Chalmers gasifier. A trace stream of He was added to the raw gas, so as to derive the flow rate of the upgraded gas exiting the reactor. The tar sampling for the upgraded gas at the outlet of the reactor was done using the same type of SPA columns as was used for sampling the tar in the raw gas. After the conditioning step to remove steam and tar, the permanent gas composition was analyzed online using the NGA gas analyzer and the micro-GC. The experiments were conducted at 800°C and for three gas-solid contact times: 0.6, 0.8, and 1.1 s. Note that the solid-gas contact time was varied by changing either the raw gas flow rate or the quantity of the ilmenite.

To identify the contributions of steam reforming, dry reforming, and hydro-cracking reactions to the catalytic gas cleaning process using ilmenite, a second experimental investigation was conducted with fresh material.

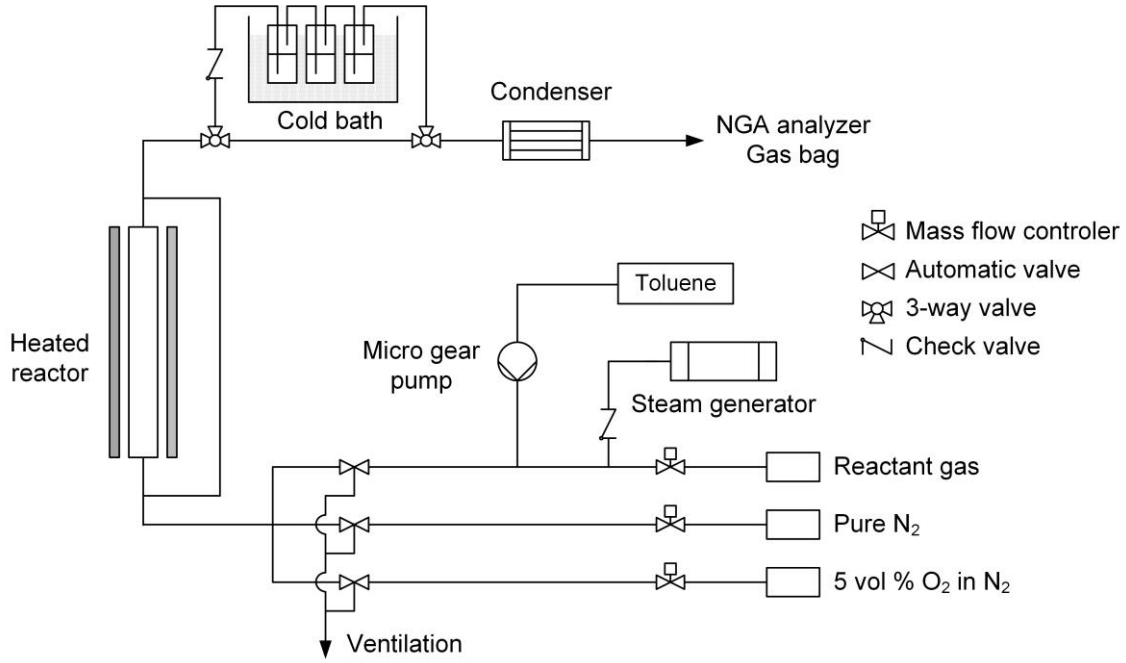

Figure 8. Experimental setup used in the investigation with synthetic reactant gases and fresh ilmenite.

The experimental setup is presented in Figure 8, with the main part being a quartz glass fluidized bed reactor. Prior to the main experiments, fresh ilmenite was activated to induce its catalytic activity. This activation was done by exposing the material to alternating oxidizing and reducing conditions at 800°C and 850°C, respectively. The experiments were performed in cycles that consisted of three successive stages, namely the reduction, inert, and oxidation stages. The reduction stage was the main focus, during which the synthetic reactant gas mixtures presented in Table 6 were fed to the reactor. The oxidation stage, which employed an oxidizing gas composed of 5 vol% O_2 diluted in N_2, was carried out to regenerate the catalyst by burning of any carbon deposited on the ilmenite particles during the preceding reduction stage. Between the reduction stage and the oxidation stage, the inert stage involved the injection of pure N_2 to flush the reactor.

Table 6. Compositions (vol%) of the reactant mixtures, details of the toluene injection, and analyses of the product gases in the different experiments.

Experiment	Composition (vol%)							Toluene injection (g/min)	Analysis
	CO	CO_2	H_2	CH_4	C_2H_4	N_2	Steam		
WGS	21.5	-	21.5	-	-	7	50	-	NGA
Ethene steam reforming	-	-	-	-	1.6	48.4	50	-	NGA, micro-GC
Gasification gas	21.5	7.5	11.5	7	2.5	-	50	-	NGA
Methane steam reforming	-	-	-	7	-	43	50	-	NGA
Toluene steam reforming	-	-	-	-	-	50	50	0.1	NGA, micro-GC, GC-FID
Synthetic raw gas	21.5	7.5	11.5	7	2.5	-	50	0.1	NGA, micro-GC, GC-FID

The experiments summarized in Table 6 were designed taking into account the composition of the raw gas produced by the Chalmers gasifier (presented in Section 5.1.2). Given the properties of the raw gas, representative reactions for the gas cleaning process were identified. More specifically, as the raw gas contains a high content of steam, WGS and steam reforming reactions were expected to play key roles. Thus, the WGS, methane steam reforming, ethene steam reforming, and toluene steam reforming reactions were studied, both independently and together with each other. In the latter case, hydro-cracking and dry reforming reactions could also occur since reactant gases contained H_2 and CO_2. The focus was on methane and ethene, as they are the main light HC in the raw gas. Toluene was chosen as tar-representative because it is one of the major tar components (see Section 5.1.2). Furthermore, benzene, which is one of the most stable tar species, can be produced from toluene, which might provide more details about the tar evolution [37]. The analyses performed in the different experiments are also summarized in Table 6. In particular for the *toluene steam reforming* experiment and *synthetic raw-gas* experiment in which toluene was injected into the reactor, the product gas that exited the reactor was led to a series of three impingers that contained 2-propanol placed in a cold bath at -8°C. The samples of 2-propanol were then collected for analysis by GC-FID, to measure the remaining toluene and other condensable organic compounds formed during the reduction stage. The results of this second experimental investigation are presented in Section 6.2.

6. Results and discussion

6.1. Evolution of tar and light hydrocarbons

Using the kinetic approach proposed in Chapter 3 and the experimental results for the process-activated ilmenite, the compositions of the different tar and light HC groups in relation to the gas-solid contact time were derived, and they are shown in Figure 9a,b and Figure 10a,b. The aggregate mole fraction of CO plus CO_2, and the aggregate mole fraction of H_2 plus steam are also presented in these figures.

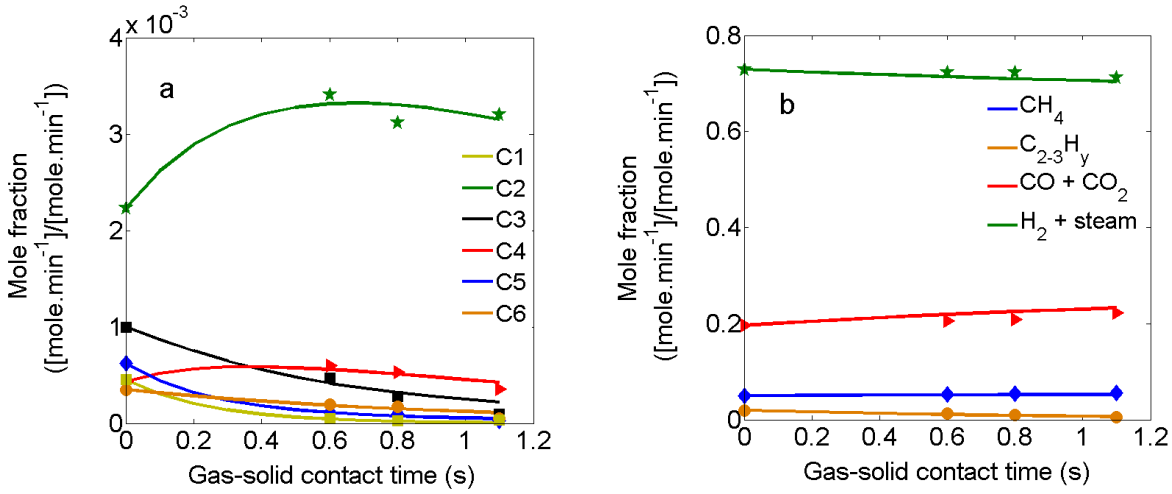

Figure 9a,b. Calculated (lines) and measured (markers) compositions of the upgraded gas in relation to increases in the gas-solid contact time.

Figure 9a,b shows the composition of the upgraded gas for a contact time of up to 1.1 s. It can be seen from Figure 9a that lower mole factions of phenolic and oxygen-containing compounds (C1), 1-ring compounds (C3), 2-ring compounds (C5), and 3-ring and larger compounds (C6) are achieved as the contact time increases. Moreover, the destruction of these tar groups produces benzene (C2) and naphthalene (C4), resulting in increases in the levels of groups C2 and C4. There is a considerable decrease in the composition of the light HC $C_{2\text{-}3}H_y$, and there is only a very small change in the level of methane, as shown in Figure 9b.

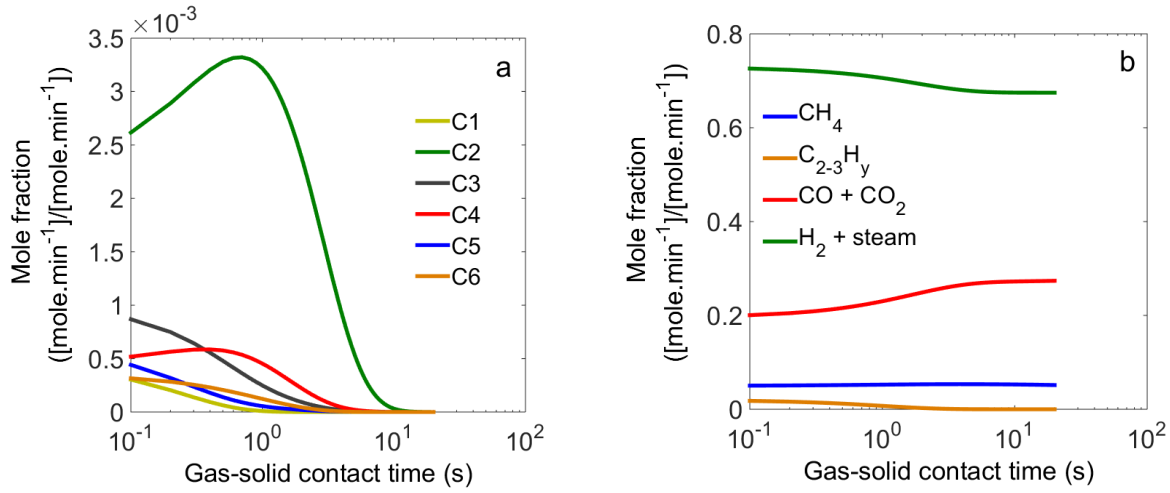

Figure 10a,b. Compositions of the upgraded gas with increases in the gas-solid contact time.

Figure 10a,b shows the compositions of the upgraded gas with increases in the gas-solid contact time (up to 20 s). Validation of the model prediction would require additional experiments at longer gas-solid contact times than those used in the present work. For a gas-solid contact time of approximately 5 s, one could expect full conversion of phenolic and oxygen-containing compounds (C1), 1-ring compounds (C3), 2-ring compounds (C5), and 3-ring and larger compounds (C6). For its complete removal, naphthalene (C4) requires a longer gas-solid contact time of approximately 6 s. Benzene (C2), which is the most abundant tar group in the upgraded gas, requires a significantly longer gas-solid contact time (approximately 12 s) to be eliminated completely. For the light HC, the $C_{2\text{-}3}H_y$ group can be completely removed with a gas-solid contact time of around 3 s, while the methane fraction remains almost constant.

From the obtained evolutionary profiles of the different tar and light HC groups, a conversion network for the tar and light HC groups can be proposed, as shown in Figure 11.

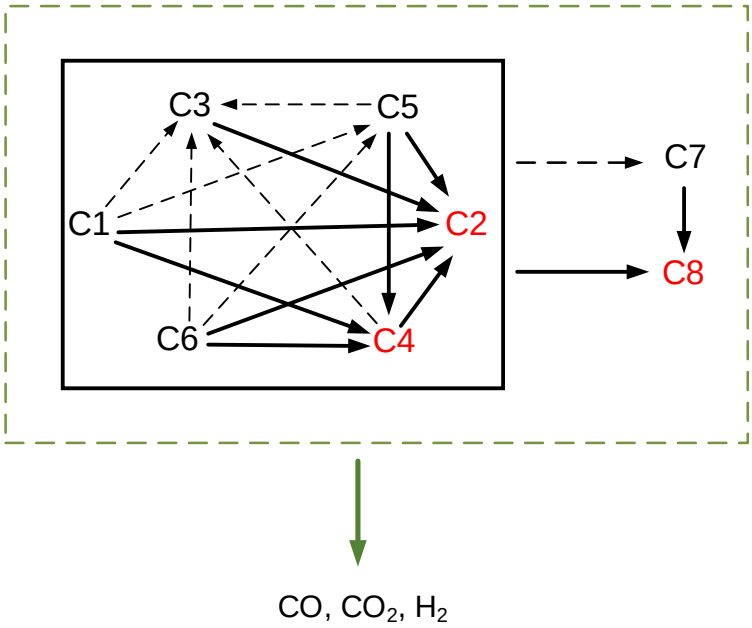

Figure 11. Conversion network for the tar and light HC groups with: C1: phenolic and oxygen-containing compounds; C2: benzene; C3: 1-ring compounds; C4: naphthalene; C5: 2-ring compounds; C6: 3-ring and larger compounds; C7: $C_{2\text{-}3}H_y$; and C8: methane.

As the raw gas contains a significantly high steam content and thus can induce a high concentration of hydrogen intermediates H^*, the formation of relatively heavier tar/HC molecules is neglected. Only the conversion pathways in which the destruction of the heavier tar/light HC groups produces relatively lighter ones are included. $C_{2\text{-}3}H_y$ and methane can be produced from all the tar groups, and the destruction of $C_{2\text{-}3}H_y$ can result in the formation of methane. Moreover, the conversion routes, which produce naphthalene, benzene and methane and are represented by the solid lines in Figure 11, are identified as being among the most important pathways.

Overall, the obtained results provide additional details about the evolution of tar and light HC in a general catalytic gas cleaning process, particularly in an environment with high steam content. Based on this, the process conditions for optimizing the formation of desired products can be determined. For a certain operating temperature, the selection of catalyst would be the most important factor. For instance, ilmenite represents a good choice if methane is a desired product after the catalytic upgrading of the raw gas. However, if CO and H_2 are the expected products, catalysts with higher catalytic activities, such as nickel catalysts, are necessary. This is also to avoid the need for extensive gas-solid contact times, which might require a large reactor volume, a large amount of catalyst, or changing of the fluidizing regime in the reactor from bubbling to circulating mode.

6.2. Contribution of decomposition reactions to catalytic gas cleaning

This section presents the main results obtained in the experiments using fresh ilmenite and synthetic reactant gas mixtures.

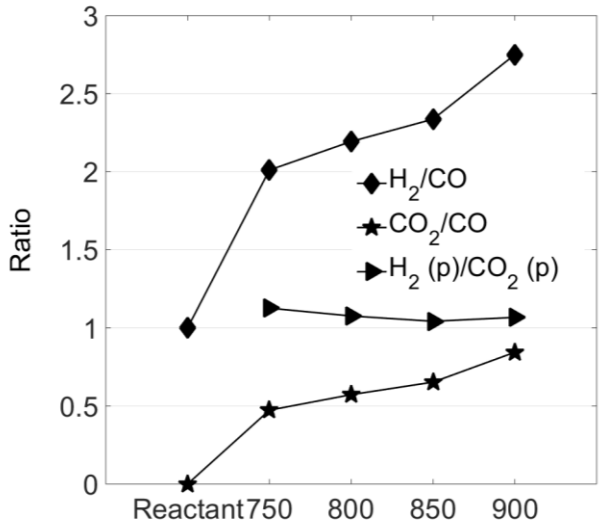

Figure 12. *WGS* experiment. Changes in the gas compositions represented by H_2/CO and CO_2/CO ratios; and H_2(p)/CO_2(p) ratio that compares the amount of H_2 produced [here termed H_2(p)] to the amount of CO_2 produced [here termed CO_2(p)].

In the *WGS* experiment, considerable levels of production of H_2 and CO_2 and consumption of CO were observed, as evidenced by the changes in gas compositions comparing the dry reactant gas and product gas, i.e., the H_2/CO and CO_2/CO ratios in Figure 12. The occurrence of the forward WGS reaction was significant and was the main reaction that induced the changes in the CO, CO_2, and H_2 levels. Indeed, the oxidizing reactions of CO and H_2 with oxygen that was possibly carried by ilmenite particles to produce CO_2 and H_2O, respectively, could be neglected as the production levels of H_2 and CO_2 were essentially equal for all the studied temperatures, as indicated by the H_2(p)/CO_2(p) ratio in Figure 12.

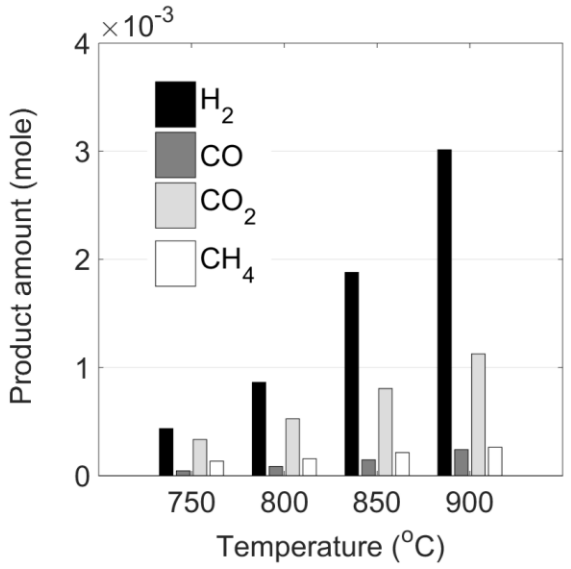

Figure 13. *Ethene steam reforming* experiment. Amounts of products achieved at different reactor temperatures.

In the *ethene steam reforming* experiment, H_2, CO, CO_2 and CH_4 were obtained in the product gas and their amounts are shown in Figure 13. The carbonaceous products CO, CO_2 and CH_4 were produced, in which the total amounts of CO and CO_2 were considerably higher than those of CH_4. This indicates that both the complete steam reforming reaction and steam dealkylation took place.

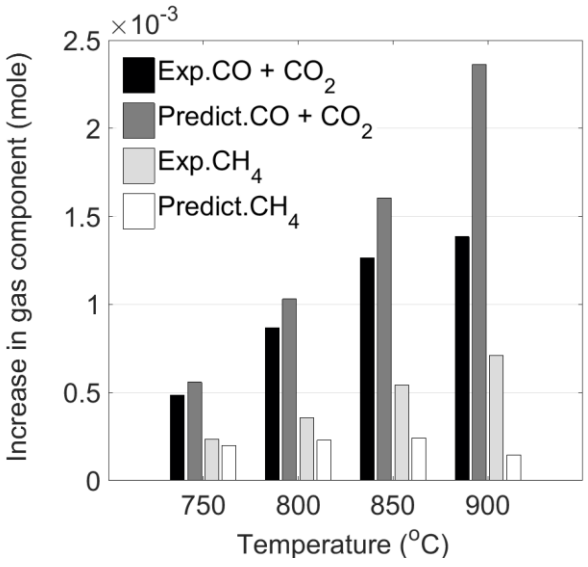

Figure 14. *Gasification gas* experiment. Experimental (Exp.) data and predicted (Predict.) data for increases in the levels of CO plus CO_2, and of CH_4 for different reactor temperatures.

In *gasification gas* experiment, increases in the levels of CO plus CO_2, and of CH_4 comparing the product gas to the reactant gas were predicted. The calculated data and the corresponding experimental data are featured in Figure 14. This was done to investigate the change in product

formation following ethene conversion in two scenarios: (i) ethene was decomposed mainly *via* steam reforming reactions; and (ii) in addition to steam reforming, ethene was decomposed *via* hydro-cracking and dry reforming reactions, which could be exacerbated by the WGS reaction, as the reactant gas mixtures contained CO, CO_2, and H_2. In general, the predicted data were calculated using the conversion efficiencies of methane and ethene obtained in the *gasification gas* experiment and the results for the distributions of carbonaceous products obtained in the *methane steam reforming* and *ethene steam reforming* experiments. It can be seen from Figure 14 that the actual increases in the levels of CO and CO_2 were lower than the predicted values, and this became more pronounced as the temperature increased. However, the opposite trend was observed for CH_4. Thus, the distribution of carbon-containing products changed towards more HC products and fewer oxidation products as H_2 appeared in the reactant gas, which indicates the effect of the hydro-cracking reaction. Although CO_2 was present in the reactant gas, the production of oxidation products did not increase. Therefore, the dry reforming reaction was not significant relative to the steam reforming and hydro-cracking reactions. It must be emphasized that in the *gasification gas* experiment the occurrence of the WGS reaction modulated the H_2 and CO_2 concentrations (see the results from the *WGS* experiment), and thus could have favored the hydro-cracking and dry reforming reactions. However, only the hydro-cracking reaction occurred to a significant extent.

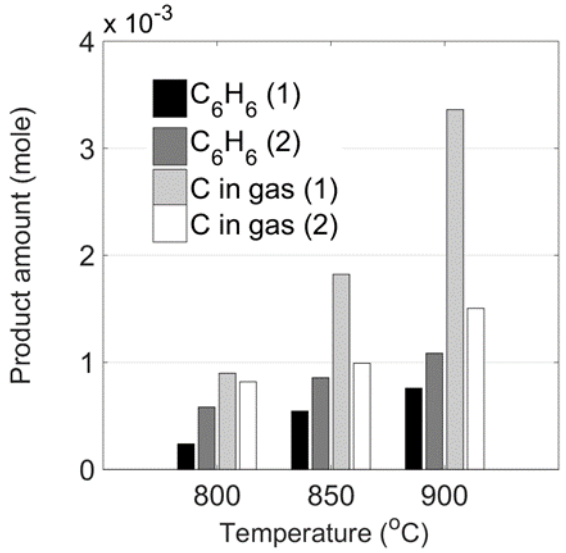

Figure 15. Amounts of benzene and of total carbon increasing in permanent product gas obtained in: (1) *toluene steam reforming* experiment, and (2) *synthetic raw gas* experiment for different reactor temperatures.

In the *toluene steam reforming* experiment, carbon-containing products CO, CO_2, CH_4, C_2H_4 and benzene were obtained in the product stream. Among these products, ethene C_2H_4 was present at insignificant level. Furthermore, the total yields of CO and CO_2 were higher compared to those of other carbon-containing products (data is not shown here). Thus, it could be implied that both the complete steam reforming reaction and steam dealkylation occurred. The amounts of benzene,

and the amounts of carbon in permanent product gases at studied temperatures 800–900°C are presented in Figure 15. The amounts of these products in *synthetic raw gas* experiment are given in the same figure. It is seen that the amounts of benzene were higher in the *synthetic raw gas* experiment than in the *toluene steam reforming* experiment. However, the amounts of carbon increasing in the permanent product gases were lower.

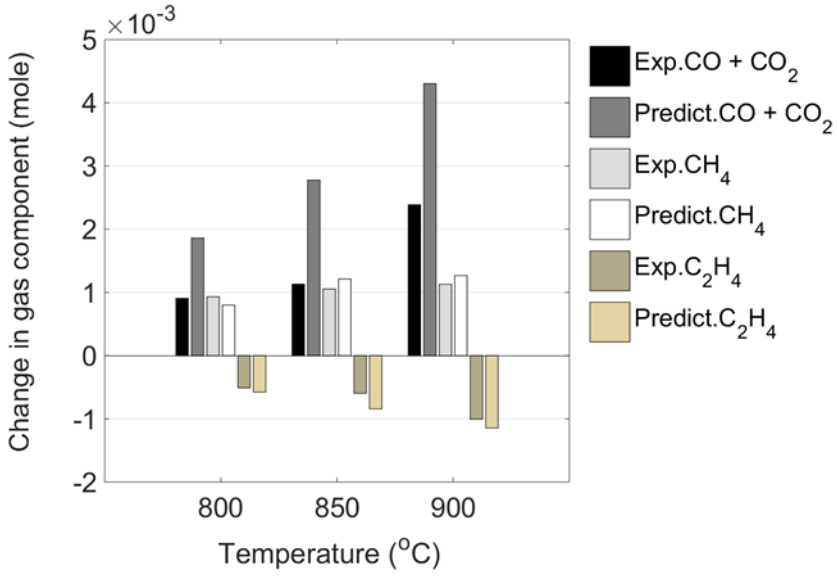

Figure 16. *Synthetic raw gas* experiment. Experimental (Exp.) data and predicted (Predict.) data for increases in the levels of CO plus CO_2, and of CH_4, and for decreases in the levels of C_2H_4 for different reactor temperatures.

For toluene conversions, cases in which H_2 and CO_2 were present or not present in the reactant gas were compared to investigate the changes in the nature of the carbonaceous products. Figure 16 shows the experimental and predicted data for the levels of CO plus CO_2, and of CH_4 increased, and the levels of C_2H_4 decreased between the reactant gas and the product gas in the *synthetic raw gas* experiment. The predicted data were calculated based on the conversion efficiencies of toluene in the *synthetic raw gas* experiment, the results for the distributions of carbonaceous products obtained in the *toluene steam reforming* experiment, and the absolute changes in the levels of gas components obtained in the *gasification gas* experiment. As shown in Figure 16, the most significant differences between the actual and predicted results were noted for CO plus CO_2, whereby the actual increases were lower than the predicted ones; and this difference was enhanced as temperature increased. This observation together with the benzene amounts presented in Figure 15 show that the production of carbonaceous products deviated towards more HC products and fewer oxidation products, as H_2 was present in the reactant gas and a significant amount of H_2 was produced by the WGS reaction. The presence of CO_2 in the reactant gas and the CO_2 produced by the WGS reaction did not direct the process towards more oxidation products. Thus, these results are in line with the results of the ethene conversions discussed previously,

which showed that the steam reforming and hydro-cracking reactions were important and the dry reforming reaction was relatively negligible.

In the conducted experiments, steam reforming reactions were expected to be the most efficient, as compared to the hydro-cracking and dry reforming reactions, given that steam represented about 50 vol% of the reactant gas. However, the presence of H_2 in the reactant gas and of H_2 produced by the WGS reaction significantly biased the forms of the products in the product gas towards more HC products and fewer oxidation products, which was accelerated following the temperature. The hydro-cracking reaction, thus, occurred to a considerable extent and was favored at higher temperature. In contrast, the presence of CO_2 or the dry reforming reaction did not generate any noticeable changes in the form of the product. Moreover, considerable production levels of methane and benzene were observed in the *ethene steam reforming* and *toluene steam reforming* experiments, respectively, even though steam was present in excess for the complete steam reforming reactions of ethene and toluene occurring exclusively. This showed the effect of steam dealkylation and revealed that the catalytic activity of ilmenite under studied conditions was not sufficient to eliminate methane and benzene. In summary, by understanding the contributions of the different decomposition reactions of tar/light HC to the overall catalytic gas cleaning process, the relative quantities of the pseudo-tar CH_mO_n and CO that are produced through the destruction of tar/light HC $C_{x_i}H_{y_i}O_{z_i}$, i.e., the w_i/x_i ratios (see Section 3.2), can be estimated in a more practical manner.

7. Conclusion

In this work, a mechanism is formulated based on reactive intermediates to describe the principal trends in the evolution of tar and light hydrocarbons during catalytic gas cleaning. Furthermore, a kinetic model is developed using the proposed mechanism and a pseudo-tar that represents the tar and light hydrocarbons formed *in situ*. The kinetic approach considers all the tar species in the raw gas, the main reaction routes, the roles of reforming/cracking agents, and the conversion of light hydrocarbons. The emphasis was on the raw gas produced by the Chalmers dual fluidized bed biomass gasifier operated at 820°C, which has a high steam content, large fractions of methane and light hydrocarbons in the range of C_2–C_3 carbons, and stable aromatic tar components. Furthermore, an ilmenite catalyst was selected to demonstrate the applicability of the kinetic model. By applying the kinetic model to process-activated ilmenite, the evolutionary profiles of different tar and light hydrocarbon groups as a function of gas-solid contact time are elucidated, and a conversion network for the tar and light hydrocarbons is proposed. The contributions of the decomposition reactions of tar and light hydrocarbons to the catalytic gas cleaning are also elucidated in this work. Particularly for ilmenite catalysis in an environment with excess steam, the steam reforming and hydro-cracking reactions are identified as the predominant routes, while the dry reforming reaction is of little importance. Moreover, in the steam reforming routes, both the complete steam reforming reaction and steam dealkylation take place.

8. Future work

To refine the kinetic model, the following future studies are recommended:

- For the ilmenite catalyst, experiments with longer gas-solid contact times than those achieved in the present work should be carried out to validate the evolutionary profiles and to elucidate the destruction of stable components, particularly naphthalene, benzene, and methane.
- Application of the kinetic approach for catalysts other than ilmenite is needed to investigate whether the approach can be adapted to another catalysts, with appropriate modifications in relation to the catalyst used.
- The thermal effect should be studied in relation to both the destruction of tar and light hydrocarbons and the *in situ* formation of tar/light hydrocarbons from CO and H_2.
- Ethene and methane are the final hydrocarbon products in the conversion network of tar and light hydrocarbons. As the concentrations of these species can be easily measured online using conventional apparatuses, the idea is to develop an approach to use these species as surrogates to predict rapidly the tar content or the progression of tar decomposition.

Abbreviations

HC, light hydrocarbons

WGS, water-gas shift (reaction)

CST, cold solvent trapping

SPA, solid phase absorption

GC-FID, gas chromatography with a flame ionization detector

References

1. E4Tech, *Review of Technologies for Gasification of Biomass and Wastes*, 2009, National Non-Food Crops Centre: United Kingdom.
2. Dayton, D., *A Review of the Literature on Catalytic Biomass Tar Destruction* 2002, National Renewable Energy Laboratory: Golden, Colorado.
3. Bridgwater, A. V., *Renewable fuels and chemicals by thermal processing of biomass.* Chemical Engineering Journal, 2003. **91**(2–3): p. 87-102.
4. Torresa, W.; Pansarea, S. S.; Goodwin, J. G., *Hot Gas Removal of Tars, Ammonia, and Hydrogen Sulfide from Biomass Gasification Gas.* Catalysis Reviews, 2007. **49**(4): p. 407-456.
5. Larsson, A.; Seemann, M.; Neves, D.; Thunman, H., *Evaluation of Performance of Industrial-Scale Dual Fluidized Bed Gasifiers Using the Chalmers 2–4-MWth Gasifier.* Energy & Fuels, 2013. **27**(11): p. 6665-6680.
6. Milne, T. A.; Evans, R. J.; Abatzoglou, N., *Biomass Gasifier "Tars": Their Nature, Formation, and Conversion*, 1998, National Renewable Energy Laboratory: Golden, Colorado.
7. Li, C.; Suzuki, K., *Tar property, analysis, reforming mechanism and model for biomass gasification-An overview.* Renewable & Sustainable Energy Reviews, 2009. **13**(3): p. 594-604.
8. Devi, L.; Ptasinski, K. J.; Janssen, F. J. J. G., *A review of the primary measures for tar elimination in biomass gasification processes.* Biomass & Bioenergy, 2003. **24**(2): p. 125-140.
9. Larsson, A.; Israelsson, M.; Lind, F.; Seemann, M.; Thunman, H., *Using Ilmenite To Reduce the Tar Yield in a Dual Fluidized Bed Gasification System.* Energy & Fuels, 2014. **28**(4): p. 2632-2644.
10. Marinkovic, J.; Thunman, H.; Knutsson, P.; Seemann, M., *Characteristics of olivine as a bed material in an indirect biomass gasifier.* Chemical Engineering Journal, 2015. **279**: p. 555-566.
11. Berdugo Vilches, T.; Thunman, H., *Experimental Investigation of Volatiles-Bed Contact in a 2-4 MWth Bubbling Bed Reactor of a Dual Fluidized Bed Gasifier.* Energy & Fuels, 2015. **29**(10): p. 6456-6464.
12. Srinivas, S.; Field, R. P.; Herzog, H. J., *Modeling Tar Handling Options in Biomass Gasification.* Energy & Fuels, 2013. **27**(6): p. 2859-2873.
13. Abu El-Rub, Z.; Bramer, E. A.; Brem, G., *Review of Catalysts for Tar Elimination in Biomass Gasification Processes.* Industrial & Engineering Chemistry Research, 2004. **43**(22): p. 6911-6919.

14. Woolcock, P. J.; Brown, R. C., *A review of cleaning technologies for biomass-derived syngas.* Biomass & Bioenergy, 2013. **52**: p. 54-84.

15. Basu, P., *Chapter 4 - Tar Production and Destruction*, in *Biomass Gasification and Pyrolysis* 2010, Academic Press: Boston. p. 97-116.

16. Singh, R. N.; Singh, S. P.; Balwanshi, J. B., *Tar removal from Producer Gas: A Review.* Research Journal of Engineering Sciences, 2014. **3**(10): p. 16-22.

17. Anis, S.; Zainal, Z. A., *Tar reduction in biomass producer gas via mechanical, catalytic and thermal methods: A review.* Renewable and Sustainable Energy Reviews, 2011. **15**(5): p. 2355-2377.

18. Yung, M. M.; Jablonski, W. S.; Magrini-Bair, K. A., *Review of catalytic conditioning of biomass-derived syngas.* Energy & Fuels, 2009. **23**(4): p. 1874-1887.

19. Kopyscinski, J.; Schildhauer, T. J.; Biollaz, S. M. A., *Production of synthetic natural gas (SNG) from coal and dry biomass-A technology review from 1950 to 2009.* Fuel, 2010. **89**(8): p. 1763-1783.

20. van Paasen, S. V. B.; Kiel, J. H. A., *Tar formation in a fluidised-bed gasifiers-Impact of fuel properties and operating conditions*, 2004, Energy Research Centre of the Netherlands.

21. Jönsson, O., *Thermal Cracking of Tars and Hydrocarbons by Addition of Steam and Oxygen in the Cracking Zone*, in *Fundamentals of Thermochemical Biomass Conversion* 1985. p. 733-746.

22. Świerczyński, D.; Libs, S.; Courson, C.; Kiennemann, A., *Steam reforming of tar from a biomass gasification process over Ni/olivine catalyst using toluene as a model compound.* Applied Catalysis B: Environmental, 2007. **74**(3–4): p. 211-222.

23. Devi, L.; Ptasinski, K. J.; Janssen, F. J. J. G., *Pretreated olivine as tar removal catalyst for biomass gasifiers: investigation using naphthalene as model biomass tar.* Fuel Processing Technology, 2005. **86**(6): p. 707-730.

24. Corella, J.; Narváez, I.; Orío, A. *Criteria for selection of dolomites and catalysts for tar elimination from gasification gas; kinetic constants*. in *VTT Symposium 163*. 1996. Finland.

25. Corella, J.; Toledo, J. M.; Aznar, M.-P., *Improving the Modeling of the Kinetics of the Catalytic Tar Elimination in Biomass Gasification.* Industrial & Engineering Chemistry Research, 2002. **41**(14): p. 3351-3356.

26. Corella, J.; Caballero, M. A.; Aznar, M.-P.; Brage, C., *Two Advanced Models for the Kinetics of the Variation of the Tar Composition in Its Catalytic Elimination in Biomass Gasification.* Industrial & Engineering Chemistry Research, 2003. **42**(13): p. 3001-3011.

27. Lind, F.; Berguerand, N.; Seemann, M.; Thunman, H., *Ilmenite and Nickel as Catalysts for Upgrading of Raw Gas Derived from Biomass Gasification.* Energy & Fuels, 2013. **27**(2): p. 997-1007.

28. Gil, J.; Corella, J.; Aznar, M. a. P.; Caballero, M. A., *Biomass gasification in atmospheric and bubbling fluidized bed: Effect of the type of gasifying agent on the product distribution.* Biomass & Bioenergy, 1999. **17**(5): p. 389-403.

29. Douglas, C. E., *Relation of Reaction Time and Temperature to Chemical Composition of Pyrolysis Oils*, in *Pyrolysis Oils from Biomass* 1988, American Chemical Society. p. 55-65.

30. Morf, P.; Hasler, P.; Nussbaumer, T., *Mechanisms and kinetics of homogeneous secondary reactions of tar from continuous pyrolysis of wood chips.* Fuel, 2002. **81**(7): p. 843-853.

31. Kinoshita, C. M.; Wang, Y.; Zhou, J., *Tar formation under different biomass gasification conditions.* Journal of Analytical and Applied Pyrolysis, 1994. **29**(2): p. 169-181.

32. Baumhakl, C.; Karellas, S., *Tar analysis from biomass gasification by means of online fluorescence spectroscopy.* Optics and Lasers in Engineering, 2011. **49**(7): p. 885-891.

33. Ahmadi, M.; Knoef, H.; Van de Beld, B.; Liliedahl, T.; Engvall, K., *Development of a PID based on-line tar measurement method – Proof of concept.* Fuel, 2013. **113**: p. 113-121.

34. Osipovs, S., *Comparison of efficiency of two methods for tar sampling in the syngas.* Fuel, 2013. **103**(0): p. 387-392.

35. Brage, C.; Yu, Q.; Chen, G.; Sjöström, K., *Use of amino phase adsorbent for biomass tar sampling and separation.* Fuel, 1997. **76**(2): p. 137-142.

36. Israelsson, M.; Seemann, M.; Thunman, H., *Assessment of the Solid-Phase Adsorption Method for Sampling Biomass-Derived Tar in Industrial Environments.* Energy & Fuels, 2013. **27**(12): p. 7569-7578.

37. Nguyen, H. N. T.; Berguerand, N.; Thunman, H., *Mechanism and Kinetic Modeling of Catalytic Upgrading of a Biomass-Derived Raw Gas: An Application with Ilmenite as Catalyst.* Industrial & Engineering Chemistry Research, 2016. **55**(20): p. 5843-5853.

38. Lind, F.; Seemann, M.; Thunman, H., *Continuous Catalytic Tar Reforming of Biomass Derived Raw Gas with Simultaneous Catalyst Regeneration.* Industrial & Engineering Chemistry Research, 2011. **50**(20): p. 11553-11562.

39. Chan, F. L.; Tanksale, A., *Review of recent developments in Ni-based catalysts for biomass gasification.* Renewable and Sustainable Energy Reviews, 2014. **38**: p. 428-438.

40. Simell, P. A.; Hepola, J. O.; Krause, A. O. I., *Effects of gasification gas components on tar and ammonia decomposition over hot gas cleanup catalysts.* Fuel, 1997. **76**(12): p. 1117-1127.

41. Ratnasamy, C.; Wagner, J. P., *Water Gas Shift Catalysis.* Catalysis Reviews, 2009. **51**(3): p. 325-440.

42. Rostrup-Nielsen, J. R., *Catalytic Steam Reforming*, in *Catalysis*, J.R. Anderson and M. Boudart, Editors. 1984, Springer Berlin Heidelberg. p. 1-117.

43. Abdoulmoumine, N.; Adhikari, S.; Kulkarni, A.; Chattanathan, S., *A review on biomass gasification syngas cleanup.* Applied Energy, 2015. **155**: p. 294-307.

44. Delgado, J.; Aznar, M. P.; Corella, J., *Calcined Dolomite, Magnesite, and Calcite for Cleaning Hot Gas from a Fluidized Bed Biomass Gasifier with Steam: Life and Usefulness.* Industrial & Engineering Chemistry Research, 1996. **35**(10): p. 3637-3643.

45. Shen, Y.; Yoshikawa, K., *Recent progresses in catalytic tar elimination during biomass gasification or pyrolysis—A review.* Renewable and Sustainable Energy Reviews, 2013. **21**(0): p. 371-392.

46. Keller, M., *Novel metal oxide bed materials for efficient solid fuel gasification and gas clean-up in fluidized beds*, 2015, Chalmers University of Technology: Gothenburg, Sweden.

47. Abu El-Rub, Z.; Bramer, E. A.; Brem, G., *Experimental comparison of biomass chars with other catalysts for tar reduction.* Fuel, 2008. **87**(10–11): p. 2243-2252.

48. Keller, M.; Leion, H.; Mattisson, T.; Thunman, H., *Investigation of Natural and Synthetic Bed Materials for Their Utilization in Chemical Looping Reforming for Tar Elimination in Biomass-Derived Gasification Gas.* Energy & Fuels, 2014. **28**(6): p. 3833-3840.

49. Zhang, S.; Asadullah, M.; Dong, L.; Tay, H.-L.; Li, C.-Z., *An advanced biomass gasification technology with integrated catalytic hot gas cleaning. Part II: Tar reforming using char as a catalyst or as a catalyst support.* Fuel, 2013. **112**: p. 646-653.

50. Hosokai, S.; Kumabe, K.; Ohshita, M.; Norinaga, K.; Li, C.-Z.; Hayashi, J.-i., *Mechanism of decomposition of aromatics over charcoal and necessary condition for maintaining its activity.* Fuel, 2008. **87**(13–14): p. 2914-2922.

51. Hosokai, S.; Norinaga, K.; Kimura, T.; Nakano, M.; Li, C.-Z.; Hayashi, J.-i., *Reforming of Volatiles from the Biomass Pyrolysis over Charcoal in a Sequence of Coke Deposition and Steam Gasification of Coke.* Energy & Fuels, 2011. **25**(11): p. 5387-5393.

52. Fuentes-Cano, D.; Gómez-Barea, A.; Nilsson, S.; Ollero, P., *Decomposition kinetics of model tar compounds over chars with different internal structure to model hot tar removal in biomass gasification.* Chemical Engineering Journal, 2013. **228**: p. 1223-1233.

53. Wittcoff, H. A.; Reuben, B. G.; Plotkin, J. S., *Chemicals from Natural Gas and Petroleum*, in *Industrial Organic Chemicals* 2012, John Wiley & Sons, Inc. p. 93-138.

54. Vreugdenhil, B. J.; Zwart, R. W. R., *Tar formation in pyrolysis and gasification* 2009, Energy Research Centre of the Netherlands: The Netherlands.

55. de Klerk, A., *Cracking*, in *Fischer-Tropsch Refining* 2011, Wiley. p. 407-440.

56. Murzin, D.; Salmi, T., *Heterogeneous catalytic kinetics*, in *Catalytic Kinetics* 2005, Elsevier Science: Amsterdam. p. 225-284.

57. Ismagilov, Z. R.; Pak, S. N., *Study of elementary reactions of free radicals formed on oxide and platinum containing catalysts.* Catalysis Letters, 1992. **15**(4): p. 353-362.

58. Taralas, G.; Kontominas, M. G.; Kakatsios, X., *Modeling the Thermal Destruction of Toluene (C7H8) as Tar-Related Species for Fuel Gas Cleanup.* Energy & Fuels, 2003. **17**(2): p. 329-337.

59. Robaugh, D.; Tsang, W., *Mechanism and rate of hydrogen atom attack on toluene at high temperatures.* The Journal of Physical Chemistry, 1986. **90**(17): p. 4159-4163.

60. Shah, Y. T.; Gardner, T. H., *Dry Reforming of Hydrocarbon Feedstocks.* Catalysis Reviews, 2014. **56**(4): p. 476-536.

61. Aldén, H.; Björkman, E.; Carlsson, M.; Waldheim, L., *Catalytic Cracking of Naphthalene on Dolomite*, in *Advances in Thermochemical Biomass Conversion*, A.V. Bridgwater, Editor 1993, Springer Netherlands. p. 216-232.

62. Golombok, M., *Steam Hydrocarbon Cracking and Reforming.* Journal of Chemical Education, 2004. **81**(2): p. 228.

63. Tamhankar, S. S.; Tsuchiya, K.; Riggs, J. B., *Catalytic cracking of benzene on iron oxide-silica: catalyst activity and reaction mechanism.* Applied Catalysis, 1985. **16**(1): p. 103-121.

64. Wei, J.; Iglesia, E., *Isotopic and kinetic assessment of the mechanism of methane reforming and decomposition reactions on supported iridium catalysts.* Physical Chemistry Chemical Physics, 2004. **6**(13): p. 3754-3759.

65. Carey, F. A.; Sundberg, R. J., *Advanced Organic Chemistry. Part A: Structure and Mechanisms* 5ed 2007, New York: Springer.

66. Min, Z.; Asadullah, M.; Yimsiri, P.; Zhang, S.; Wu, H.; Li, C.-Z., *Catalytic reforming of tar during gasification. Part I. Steam reforming of biomass tar using ilmenite as a catalyst.* Fuel, 2011. **90**(5): p. 1847-1854.

67. Henderson, M. A., *The interaction of water with solid surfaces: fundamental aspects revisited.* Surface Science Reports, 2002. **46**(1–8): p. 1-308.

68. van der Laan, G. P.; Beenackers, A. A. C. M., *Intrinsic kinetics of the gas–solid Fischer–Tropsch and water gas shift reactions over a precipitated iron catalyst.* Applied Catalysis A: General, 2000. **193**(1–2): p. 39-53.

69. Zou, C.; van Duin, A. T.; Sorescu, D., *Theoretical Investigation of Hydrogen Adsorption and Dissociation on Iron and Iron Carbide Surfaces Using the ReaxFF Reactive Force Field Method.* Topics in Catalysis, 2012. **55**(5-6): p. 391-401.

70. Adánez, J.; Cuadrat, A.; Abad, A.; Gayán, P.; Diego, L. F. D.; García-Labiano, F., *Ilmenite activation during consecutive redox cycles in chemical-looping combustion.* Energy & Fuels, 2010. **24**(2): p. 1402-1413.

71. Corcoran, A.; Marinkovic, J.; Lind, F.; Thunman, H.; Knutsson, P.; Seemann, M., *Ash Properties of Ilmenite Used as Bed Material for Combustion of Biomass in a Circulating Fluidized Bed Boiler.* Energy & Fuels, 2014. **28**(12): p. 7672-7679.

72. Thunman, H.; Lind, F.; Breitholtz, C.; Berguerand, N.; Seemann, M., *Using an oxygen-carrier as bed material for combustion of biomass in a 12-MWth circulating fluidized-bed boiler.* Fuel, 2013. **113**: p. 300-309.

73. Israelsson, M.; Berdugo Vilches, T.; Thunman, H., *Conversion of Condensable Hydrocarbons in a Dual Fluidized Bed Biomass Gasifier.* Energy & Fuels, 2015. **29**(10): p. 6465-6475.